Hence over a region of one square kilometer (10^6 m^2) the present medium contains below the surface about 7 joules of radiant energy in the blue-green wavelength interval in scattered or directly transmitted form. Observe by (98) that nearly 95% of this radiant energy is stored within the first three diffuse attenuation lengths below the surface, i.e., within $3/K = 3/.169 = 17.7$ meters of the surface. Equation (98) shows how U(z) can be estimated if the net influx of radiant energy over the depth interval [0,z] is known, along with the volume absorption coefficient a. Further discussion of light storage phenomena in natural waters is given in Sec. 5.13.

1.5 Some Properties of Artificial Light Fields in Natural Waters

Artificial light fields in seas and lakes are produced by men seeking to illuminate natural underwater environs to carry out search or detection procedures, to study biological processes, or to establish techniques of underwater communication by means of residual and scattered radiant flux. To facilitate these activities some knowledge is desirable of the general quantitative relations between the optical properties of a medium and the light fields produced in that medium by various artificial sources. Such sources commonly range from those that produce highly collimated beams to those that produce conical beams of varying spread, up to uniform point sources. In this section we shall discuss several interesting empirical relations developed for artificial light fields.

Useful models of artificial light fields, which can completely elucidate the empirical findings presented below, may be based on the diffusion models discussed in Chapter 6, in particular in Secs. 6.5-6.7. However, we shall concentrate in this brief survey of artificial light fields only on the diffusion model (27) of Sec. 1.3, as it affords a simple yet adequate base on which to rest the empirical formulas.

The Pure Absorption Case

To see what the difficulties are in describing artificial light fields in the sea, suppose for the moment that sea water or any other natural hydrosol only absorbed radiant flux, and therefore did not scatter it. Suppose that a spherical source S of radius r_o, as in Fig. 1.59, has a uniform inherent surface radiance N_o. Then the apparent radiance N_r of this source's surface is:

$$N_r = N_o e^{-ar} \tag{1}$$

where a is the volume absorption coefficient of the medium. The radiant flux output P_o of the source is:

$$P_o = (4\pi r_o^2)\pi N_o \tag{2}$$

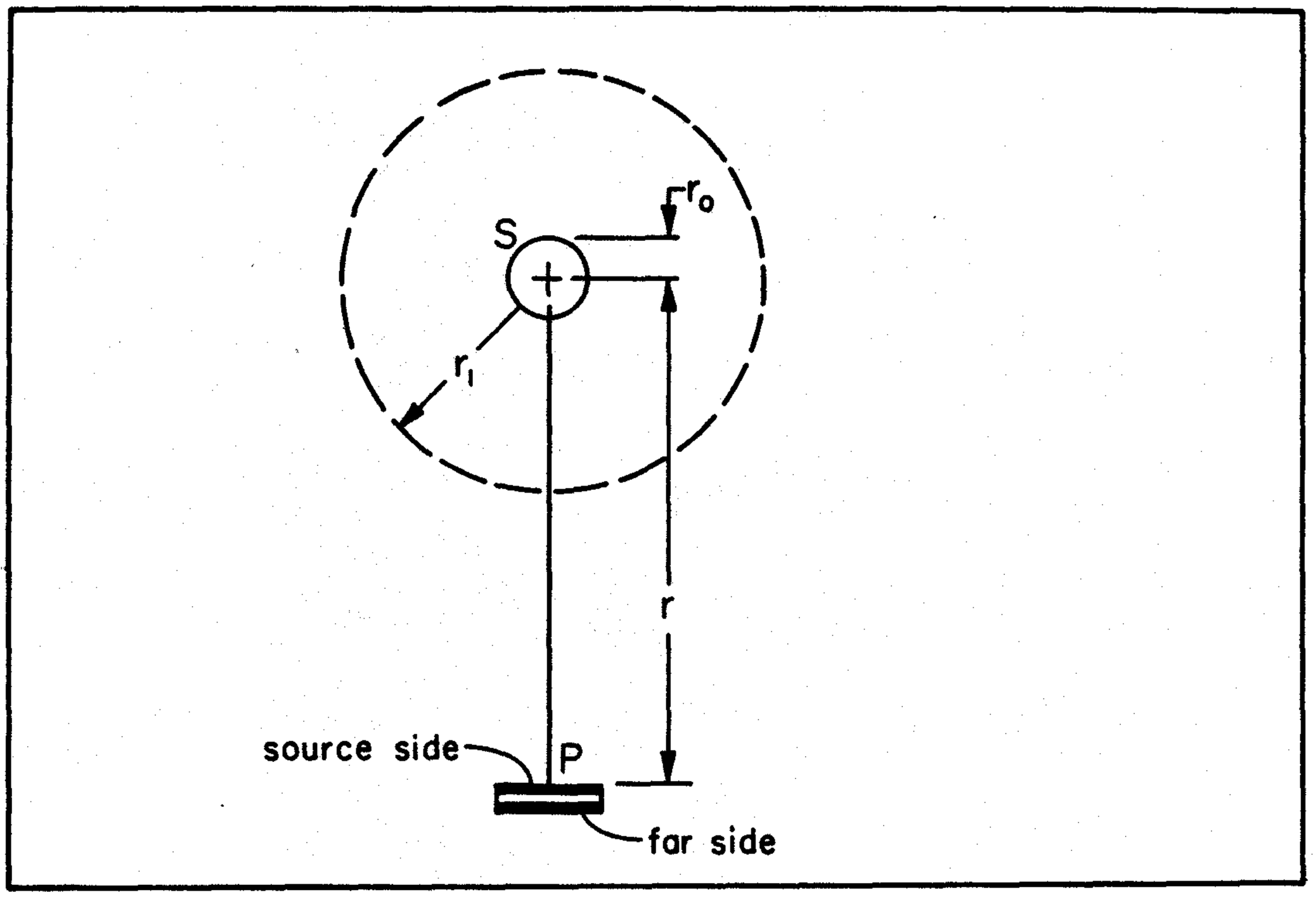

FIG. 1.59 For the derivation of the diffuse light field at P as generated by a small source S via secondary sources limited to the sphere of radius r_1. (Diffusion Model)

Its radiant intensity is:

$$J_o = \frac{P_o}{4\pi} = (\pi r_o^2)N_o \quad , \tag{3}$$

and the apparent irradiance H_r produced by the source is very nearly:

$$H_r = \frac{J_o e^{-a(r-r_o)}}{r^2} \tag{4}$$

for all $r \geq r_o$. The apparent radiance N_r and apparent irradiance H_r in the case of pure absorption are thus quite simply described because of the absence of scattered flux. Even in the present case all is not simple if the radius r_o is large compared to the absorption length $1/a$ of the medium, for then a relatively complicated integration over direction space must replace (4). However, for $r_o < 1/2a$, (4) is an adequate approximation in normal practice.

Derivation of the Semi-empirical Diffusion Model for Point Sources

When scattering may take place in the medium and to an extent in which the simple formulas (1), (4) no longer adequately describe the apparent radiance and irradiance fields,

we may go on to adopt the next simplest available model for these fields. The required candidate takes the form of (36) of Sec. 1.3 in which the integration in (37) of Sec. 1.3 is no longer over the entire space X but is restricted to a relatively small spherical region of radius r_1 about the luminous source. It is in this spherical region where the primary scattered radiant flux from the source initiates the principal part of the diffuse light field measured at relatively great distances r. The smaller r_o and r_1 are, compared to r, the more nearly will the scalar irradiance h(r) at a distance r from the source S be given by an equation of the form:

$$h(r) = h^{o}(r) + h^{*}(r)$$

$$= \frac{AJ_o e^{-\alpha r}}{r^2} + \frac{BJ_o e^{-\kappa r}}{Dr} \qquad (5)$$

where A and B are generally functions of r, or at the very least, constants used to adjust the formula to fit empirical data. It is necessary to introduce A and B because we have sidestepped integrations which could contribute measurable deviations from the simple form (5) for small and large r. We have simply used (4) above and (33) of Sec. 1.3 in a linear combination to obtain (5). A further simplification in the model can be effected if we replace κ, the decay constant indigenous to diffusion theory (cf. (32) of Sec. 1.3), by the more readily empirically determined diffuse attenuation coefficient K obtained from irradiance measurements in the sea. (K is the empirical counterpart to the k of the two-flow model discussed above.) Thus, from (32) of Sec. 1.3 we have:

$$\kappa^2 = \frac{a}{D}$$

From (92) of Sec. 1.4 we can approximate a by the form:

$$a \cong \frac{K}{D_-}$$

where D_- is now the distribution factor for the irradiance measured at point P of Fig. 1.59 produced by flux on the source side of the collector at P. If we identify κ and K, then the two preceding relations yield an estimate of the classical diffusion constant D:

$$D = \frac{1}{D_- K} \qquad (6)$$

Using this in (5), dividing each side of (5) by D_-, and keeping A, B arbitrary, we have:

$$\boxed{H(r) = J_o\left(A\,\frac{e^{-\alpha r}}{r^2} + B\,\frac{Ke^{-Kr}}{r} \right)} \qquad (7)$$

which is the desired semi-empirical form for the irradiance H(r) produced at distance r from a point source of radiant intensity J_o. α is the volume attenuation coefficient for the medium and K is the diffuse attenuation coefficient for the medium. Observe also that in passing to (7) we have dropped as negligible the irradiance on the far side of the surface at P in Fig. 1.59. Despite this conglomeration of assumptions, (7) nevertheless provides a suitable model for H(r) under judicious choice of the A and B as dictated by actual sample measurements of H(r) in real media. We shall now consider two such particular empirical forms of (7).

Two Examples of the Empirical Diffusion Model

Duntley reports in [76] and [77] the results of his empirical study during the summer of 1959 of irradiance fields produced by point sources in Lake Winnipesaukee, N.H.. He determined A and B in (7) in such a way that the resultant empirical formula should be applicable to a large set of natural hydrosols in which are imbedded point sources with a wide range of angular beam spreads.

In the case of a point source with a directionally uniform radiance over all directions, Duntley found that in (7), the constants A, B may be given by:

$$A = 1 \tag{8}$$

$$B = 2.5[1 + 7e^{-Kr}]/4\pi \tag{9}$$

This shows that for relatively small r, B is on the order of 8 times that for large r. A comparison of a real irradiance field (black dots) with that predicted by (7) using (8), (9) (solid curve) is given in Fig. 1.60. The radiant flux wavelengths measured in this experiment were via a Wratten No.61 green filter. The corresponding attenuation length of the water was $1/\alpha = 1.52$ meters, (= 5.00 feet) associated with an $\alpha = .655/m$ (= .200/ft). The K for the same water and wavelength range was found to be .187/m (= .057/ft.).

In a more detailed analysis of the empirical results, Duntley generalized (9) to include the effects of the beam spread of the source, particularly for wide beam spreads. It was found that:

$$A = 1 \tag{10}$$

$$B = \left[2.5-1.5\ \log_{10}\left(\frac{2\pi}{\beta}\right)\right]\ \left[1+7\left(\frac{2\pi}{\beta}\right)^{1/2} e^{-Kr}\right] \Big/ 4\pi \tag{11}$$

Here the point source is emitting a beam in the form of a circular cone with total angular opening of β. Observe how (11) reduces to (9) for the case of $\beta = 2\pi$. Formula (11) is expected to be a good approximation in the range $\pi/9 \leq \beta \leq 2\pi$, i.e., for all beam spreads not less than about 20°.

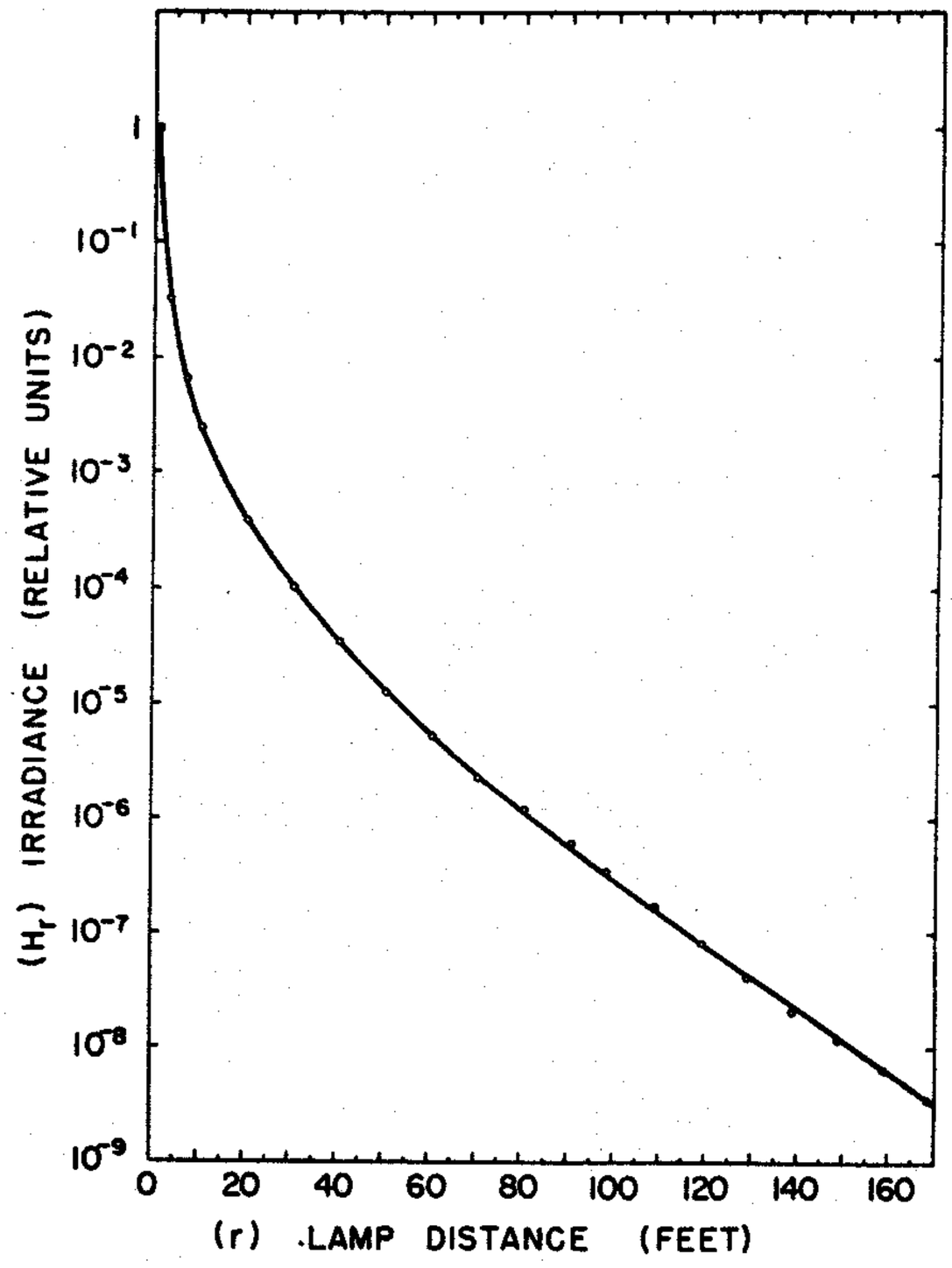

FIG. 1.60 Comparison of calculated irradiance and measured irradiance induced by a point source (small spherical lamp) by Duntley, Lake Winnipesaukee, N.H., 26 August 1959. (Fig. 16 from [78], by permission)

Radiance Distribution Produced by a Submerged Uniform Point Source

In the same set of experiments leading to the empirical determination of the diffusion model (7), (8), (9), Duntley examined the radiance distribution produced at various distances by a submerged point source of nearly uniform radiant intensity. This radiance distribution can be observed and photographed as a function of the direction from the source for various choices of the on-axis distance from the source. For nearby locations, the source (in the form of a spherical lamp) stands out sharply from its luminous halo. As viewing distance increases, the bright disk of the lamp rapidly becomes angularly smaller and also dimmer. Eventually the disk itself vanishes at about 18 to 20 attenuation lengths (i.e., at about $18/\alpha$ to $20/\alpha$ meters), but the luminous glow persists for relatively great distances. Fig. 1.61 depicts the radiance distributions produced by a point source, for a selected set of distances from the source. The lamp was a 1000 watt incandescent "diving lamp", whose 3 inch (7.62 cm) diameter spherical lamp envelope was sprayed with a lacquer to insure that its radiant intensity was uniform.

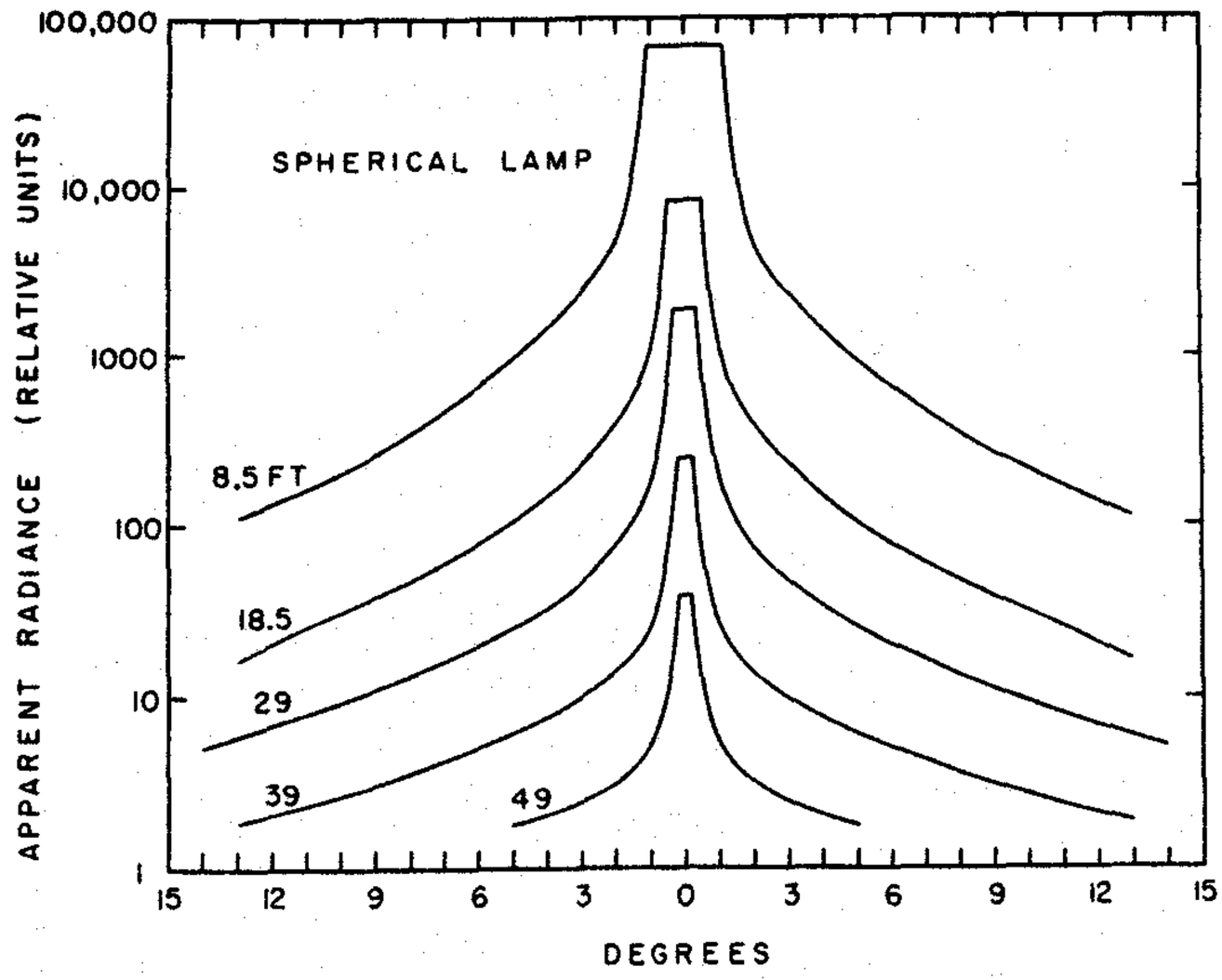

FIG. 1.61 Radiance distributions produced by a point source (small spherical lamp). Measured by Duntley, Lake Winnipesaukee, N.H., 3 August 1961. (Fig. 15 from [78], by permission)

An Empirical Study of Light Fields Produced by Collimated Sources

In the future it is likely that the laser will be used to some extent in underwater communications. It is therefore of interest to study the properties of propagation of highly collimated beams of radiant flux in natural hydrosols. In some preliminary studies in this direction, Duntley [78] had designed and constructed a source of highly collimated radiant flux, shown schematically in Fig. 1.62. Using a lens system designed by J. J. Rennilson, it was possible to produce a long, narrow, very nearly cylindrical beam of light with total beam spread 2ψ as small as 0.01° or 0.00017 of a radian. Smaller beams would begin to be noticeably spread by diffraction effects. By selecting various external beam stops it was possible to produce fine cylindrical beams of variable diameters D which were nearly divergenceless (i.e., cylindrical) over a distance $c = D/\psi$. (The figure gives the ray-geometrical significance of this relation.) Over this range the beam's residual irradiance is essentially free from inverse square effects and is of magnitude $H_r^o = H_o e^{-\alpha r}$, where $r \leq c$, $H_o = J_o/c^2$, and where J_o is the radiant intensity of the lamp used in the collimator. For distances r greater than c, the light beam would depart from its cylindrical shape and thus the residual irradiance of the beam would begin to fall off as the inverse square of r and also be further damped exponentially, so that for $r \geq c$, assuming negligible diffraction effects, we have:

$$H_r^o = \frac{H_o e^{-\alpha r}}{(r/c)^2} \quad . \qquad (12)$$

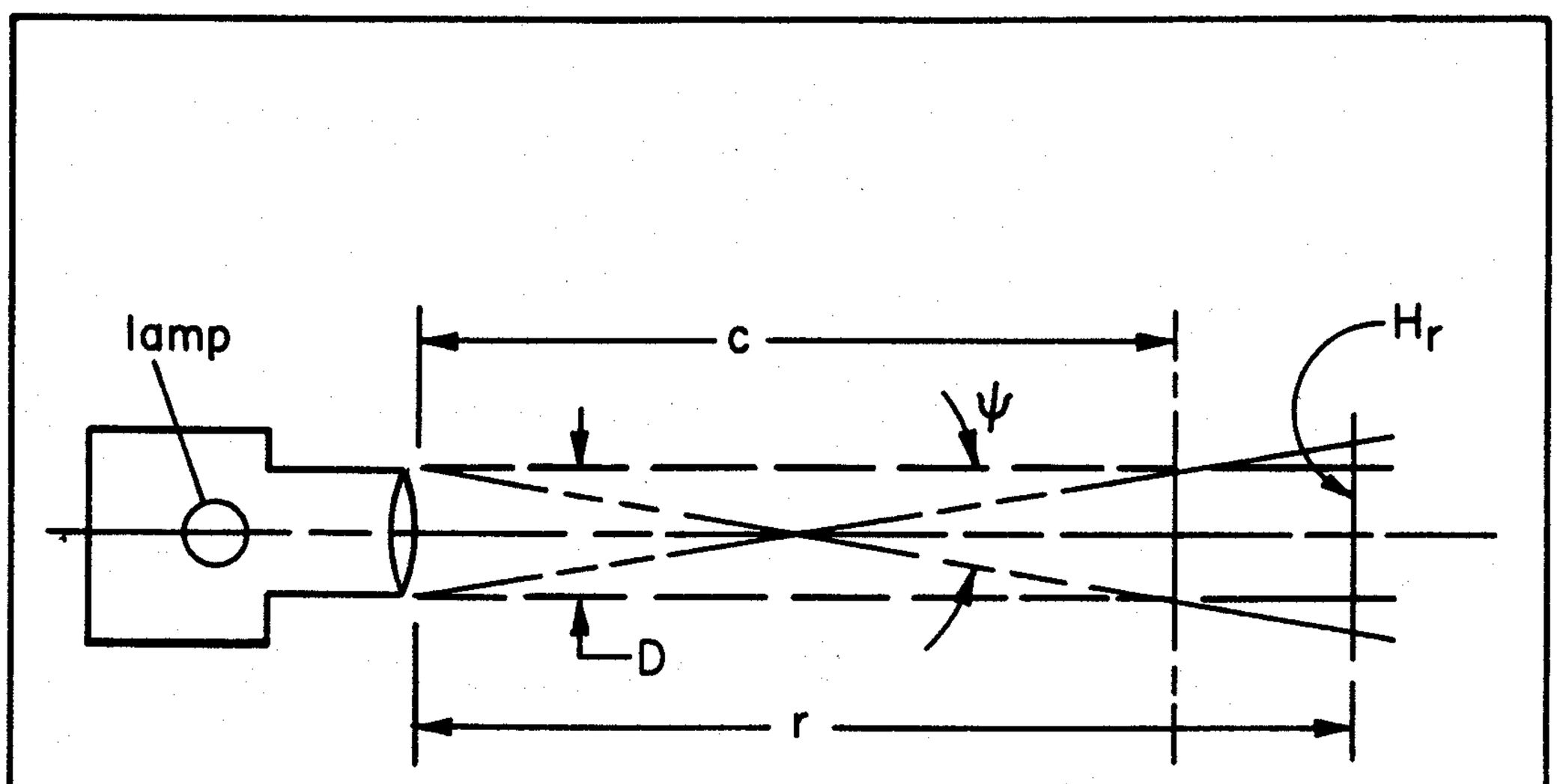

FIG. 1.62 Source for highly collimated beam of radiant flux experiment recorded in Fig. 1.63.

FIG. 1.63 Three determinations of irradiance produced by a highly collimated beam of radiant flux, as made by Duntley in Lake Winnipesaukee, N.H., 14 August 1961. (Fig. 18 from [78], by permission)

Figure 1.63 records three experimental determinations by Duntley of the apparent irradiance H_r of a highly collimated beam of spread 1/6°. The irradiance is that produced at a point on the axis of the beam a distance r from the source, and on a plane normal to the axis. The experimental results were reduced so that the beam diameters D in each of the three cases are in terms of the attenuation lengths of the medium namely 1/300, 2/300 and 8/300 attenuation lengths. In this way it is possible to free the results somewhat from the nature of the particular medium in which they were found. The medium in this case was Lake Winnipesaukee, N.H. whose α was .520/m (= .158/ft.) and whose corresponding attenuation length therefore was $1/\alpha$ = 1.92 meters (= 6.3 ft.), for the wavelength band provided by Wratten No. 61 green filters. The solid lines in Fig. 1.63 are the empirically found H_r values. The dashed lines are the residual irradiances H_r^o computed from (12). The dashed lines depart from the solid lines at the points shown by triangles. These points are located at the distances $c = D/\psi$, which are 1.15 and 2.30 attenuation lengths for the 1/300 and the 2/300 curves, respectively. The point for the 8/300 beam is located 9.20 attenuation lengths away and is not shown. Hence the vertical separation of a

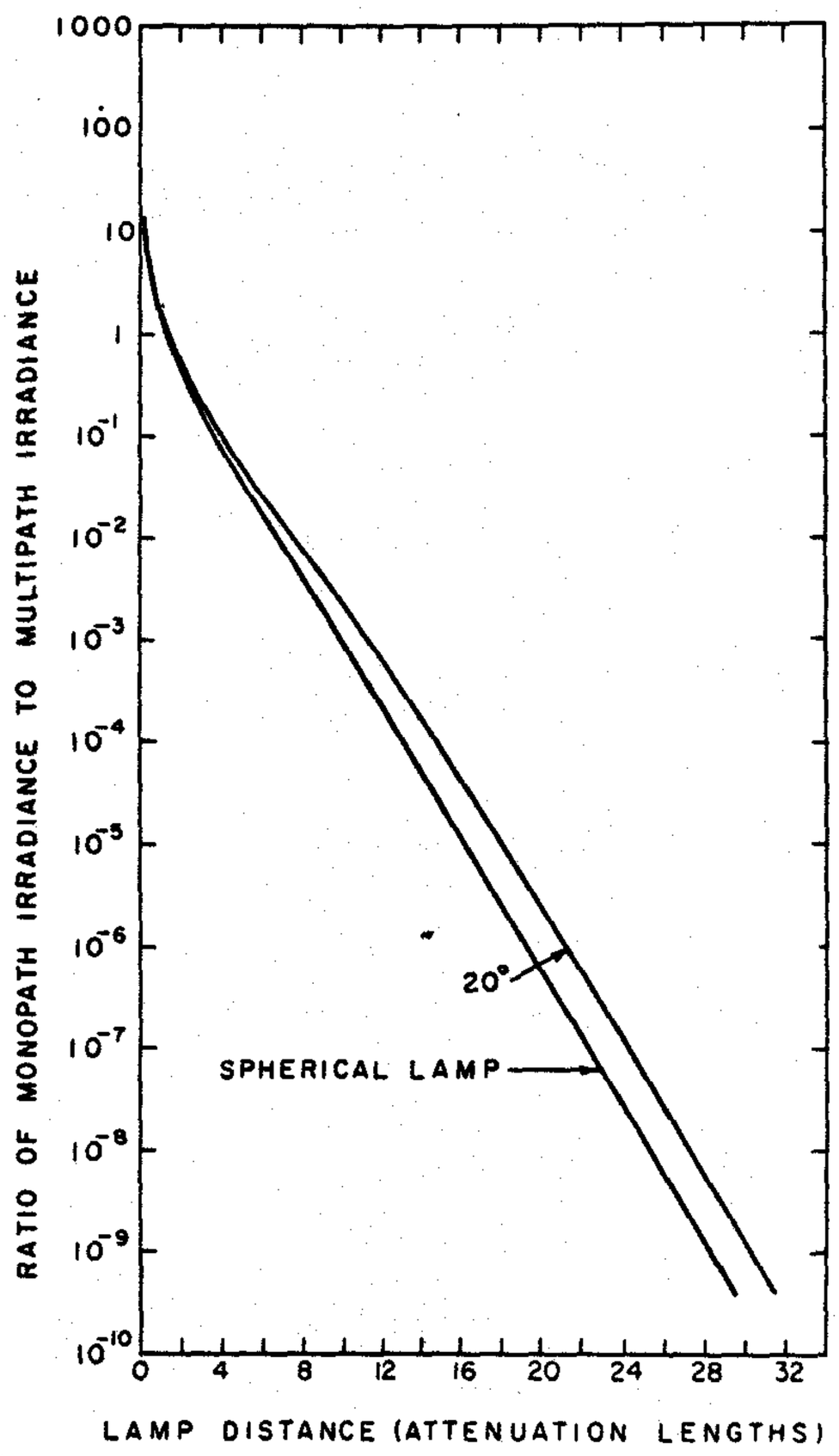

FIG. 1.64 Ratio of monopath (i.e., residual) radiance to multipath (i.e., scattered) radiance for two types of source as measured by Duntley in Lake Winnipesaukee, N.H., 26 August 1961. (Fig. 19 from [78], by permission)

solid curve and its dashed mate gives a measure of the scattered (or diffuse) irradiance H_r^* for each distance r. It should be observed that the data in Fig. 1.63 pertain only to the axis of an aplanatic underwater projection system having a beam spread of 1/6°. In other words the 1/6° beam spread cannot be scaled up and down by factors of 10. Separate and new measurements for different spreads ψ must be made to see how H_r^* depends on ψ.

Some further information on the relative magnitudes of unscattered and scattered irradiances H_r^o (monopath) and H_r^* (multipath) is given in Fig. 1.64, and is also due to Duntley [78]. The ratio H_r^o/H_r^* is plotted versus r for two cases: a spherical point source, and a point source having a total spread of 20°. In the latter case the irradiance is located on-axis and falls on a plane normal to the axis, as usual. As expected, for each fixed distance r, there is relatively more diffuse irradiance H_r^* in the case of the spherical source as for the narrow beam source. These curves are for the medium described in Fig. 1.60. The residual irradiance H_r^o was calculated using the first term of (7) with A = 1. H_r^* was obtained via $H_r - H_r^o = H_r^*$ using the irradiance H_r of Fig. 1.60 for the spherical case, and using recorded H_r data for the 20° case.

Figure 1.65 shows still another experimental finding by Duntley [78] concerning the irradiance produced by collimated beams. In this case the beam had a 2ψ of .046°, and a 2 inch (or 5.08 cm) diameter D. The medium had an α of .685/m (= .209/ft) and hence an attenuation length $1/\alpha$ of 1.46 meters

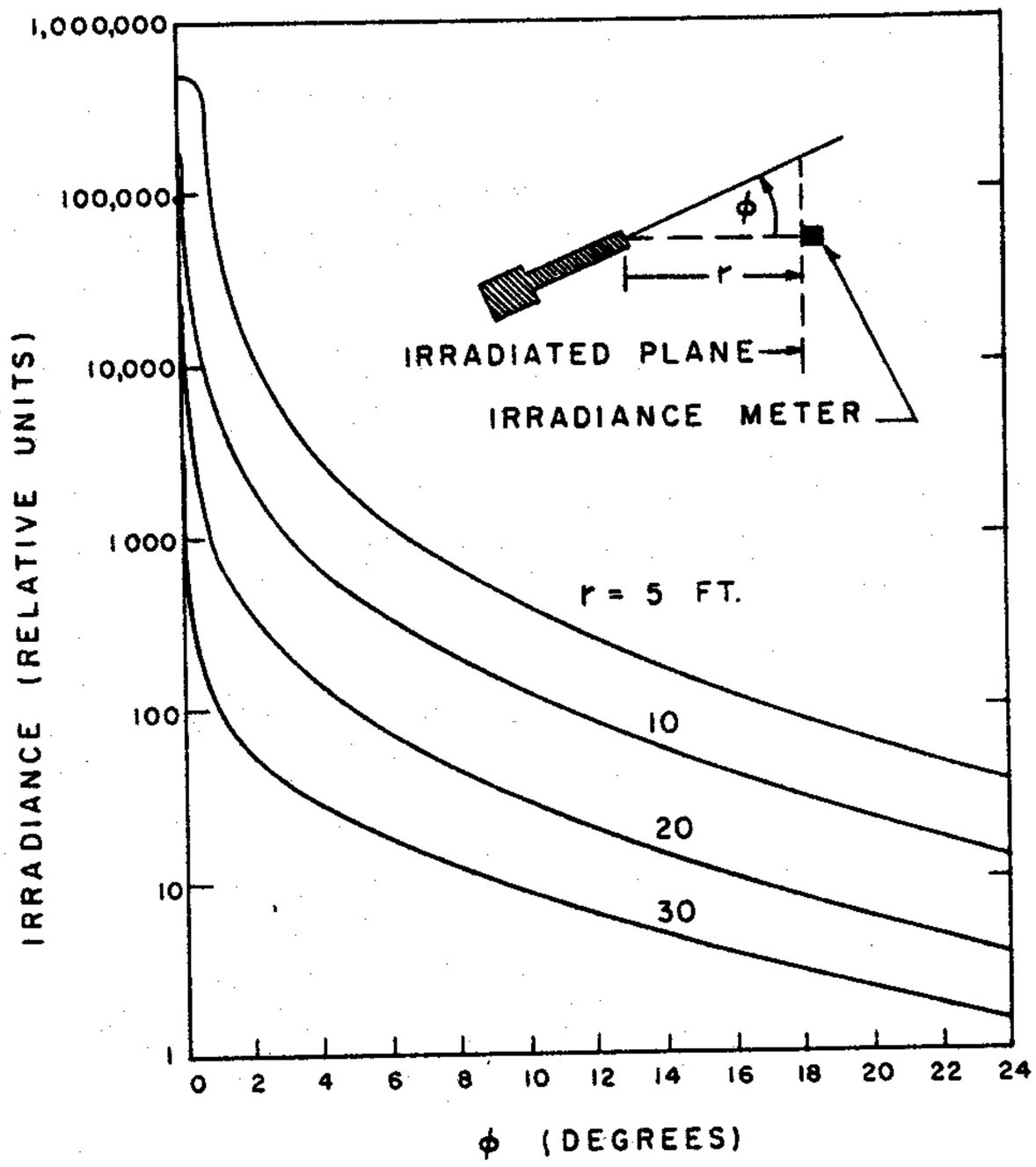

FIG. 1.65 Irradiance on a collecting plane produced by a sweeping collimated beam, as observed by Duntley, Lake Winnipesaukee, N.H., Summer 1961. (Fig. 20 from [78], by permission)

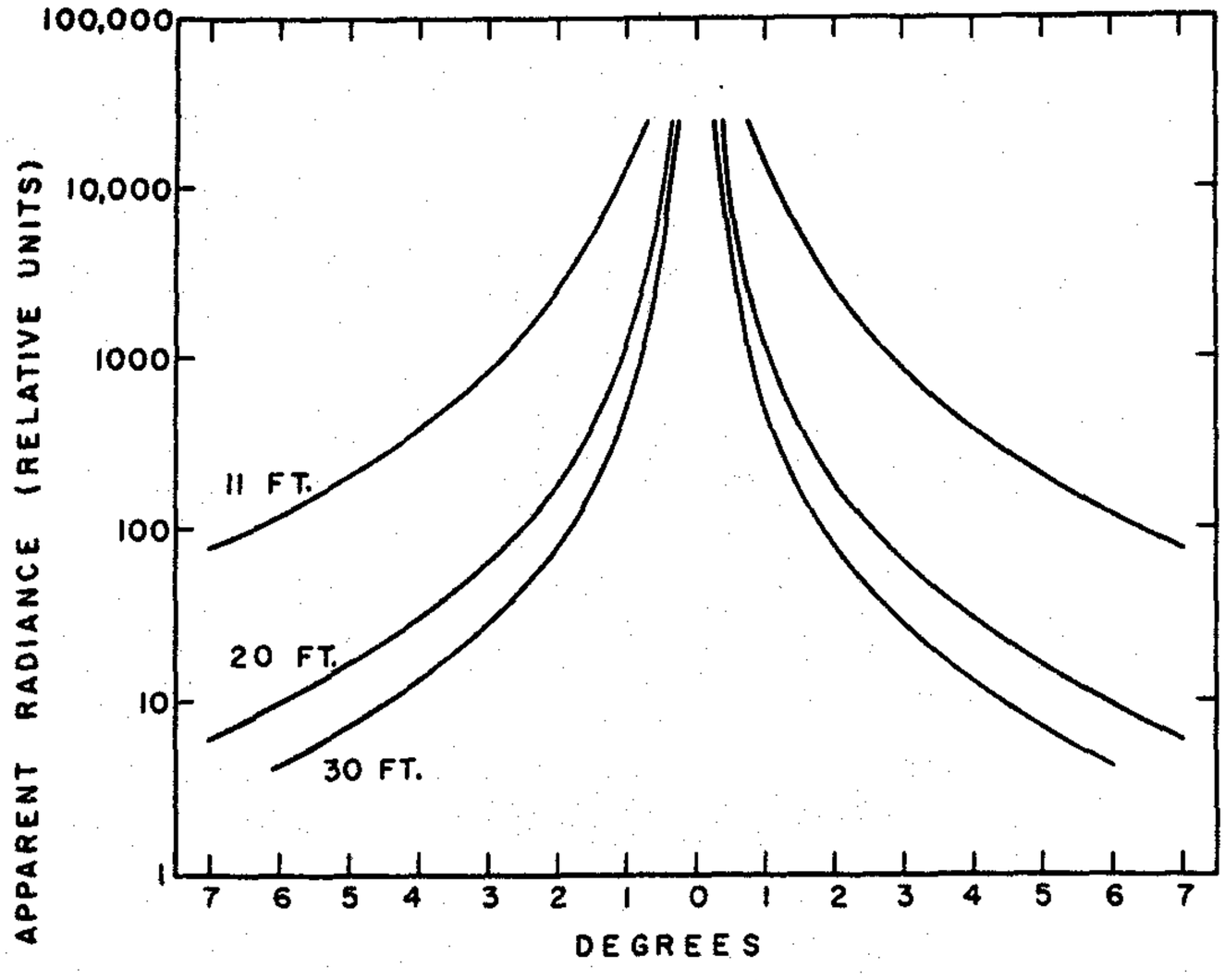

FIG. 1.66 Apparent radiance produced by beam of highly collimated flux (cf. Fig. 1.62), as found by Duntley, Lake Winnipesaukee, N.H., 11 August 1961. (Fig. 17 from [78], by permission)

(= 4.80 ft.) as measured via a Wratten No. 61 green filter, in Lake Winnipesaukee, N.H., summer, 1961. The locations of the measurements within the induced light field are indicated by the inset of the figure. The irradiated plane was swept by the moving beam.

Finally, Fig. 1.66 depicts the apparent radiance as observed under somewhat the same general test condition of Fig. 1.65. Now the beam had a 2ψ of 0.01° and was directed toward the telephotometer so that it completely filled the entrance pupil of the latter at all times. The water was slightly clearer in the present case, having an attenuation length of 2.04 meters (= 6.70 ft.), i.e., an α of .490/m (= .149/ft.) for the same wavelength band. It is of interest to compare Figs. 1.61 and 1.66, which reveal subtle differences between the radiance distributions found by looking at distant point sources and down the barrel of a collimated beam.

Some further discussion of these empirical findings, especially their applicability to underwater communications by scattered light, may be found in [79].

<< Table of Contents << Title Page >> Next Page >>

1.6 Inherent and Apparent Optical Properties of Hydrosols

The three simple models describing light fields in the seas and lakes of the earth, as developed in Sec. 1.3, may now be considered as reasonably established descriptions of radiative transfer in natural hydrosols. For as we have seen in our brief survey of their applications in Sec. 1.4 and 1.5, they can be used both to organize our accumulated empirical knowledge of natural light fields by means of faithful symbolic representations of our observations, and also to encourage, via simple mathematical manipulations, the exploration of